

AN EFFICIENT STRATEGY TO SELECT TARGETS FOR GAS-DYNAMICAL MEASUREMENTS OF BLACK HOLE MASSES USING THE *HUBBLE SPACE TELESCOPE*¹LUIS C. HO², MARC SARZI^{3,4}, HANS-WALTER RIX³, JOSEPH C. SHIELDS⁵, GREG RUDNICK⁶, ALEXEI V. FILIPPENKO⁷, AND AARON J. BARTH^{8,9}*To appear in Publications of the Astronomical Society of the Pacific.*

ABSTRACT

Gas-dynamical studies using the *Hubble Space Telescope* are an integral component for future progress in the search for massive black holes in galactic nuclei. Here we present an extensive set of gas rotation curves obtained with the Space Telescope Imaging Spectrograph for the central regions of 23 disk galaxies. We find that the bulges of randomly selected, nearby spiral and S0 galaxies generally do not contain well-defined gaseous disks. Only 15%–20% of disk galaxies have regular, symmetric velocity fields useful for dynamical analysis. Through comparison of the kinematics with *Hubble Space Telescope* images of the nuclear regions, we show that the probability of success can be significantly boosted by preselecting objects whose central dust lanes follow a well-ordered, circularly symmetric pattern. The dust morphology can be ascertained efficiently by visual inspection of unsharp-masked images.

Subject headings: galaxies: bulges — galaxies: ISM — galaxies: kinematics and dynamics — galaxies: nuclei — galaxies: spiral — galaxies: structure

1. INTRODUCTION

The installation of the Space Telescope Imaging Spectrograph (STIS; Leitherer et al. 2001) on the *Hubble Space Telescope* (*HST*) ushered in a new era in the search for massive black holes (BHs) in galactic nuclei. By now, sufficiently large numbers of BH candidates are known that the emphasis has shifted from detections of individual objects to demographic studies using statistical samples (e.g., Richstone et al. 1998; Ho 1999; Gebhardt et al. 2000b; Ferrarese & Merritt 2000). Future progress will focus on two fronts, first on sharpening the analysis techniques to improve the accuracy of the mass measurements, and second on substantially enlarging the existing samples to cover galaxies across the Hubble sequence.

BH searches with *HST* use either stars or gas to trace the central potential. These two approaches are complementary, each with its merits and limitations. Modern, fully general, stellar-dynamical models are powerful because they give information not only on masses but also on the orbital structure of the galaxy (e.g., van der Marel et al. 1998; Cretton & van den Bosch 1999; Gebhardt et al. 2000a). One drawback is that both the data and the computational requirements are expensive. Another is that the modeling can be very challenging for complicated dynamical structures; the double nucleus of M31 serves as a good illustration (e.g., Kormendy & Bender 1999; Bacon et al. 2001). This technique also cannot easily cope with dusty galaxies, as a consequence of which most stellar-dynamical work with *HST* has been biased toward early-type (mostly elliptical) galaxies.

Gas kinematics in principle offer a more straightforward measure of the central mass, provided that the gas participates

in Keplerian rotation in a disklike configuration. The observations are less demanding because optical emission lines from ionized gas generally have much higher equivalent widths than stellar absorption lines. Moreover, as demonstrated later in this paper, optical nebular emission invariably traces nuclear dust features. This technique, therefore, can be applied to galaxies inaccessible to stellar observations. Unlike stars, however, gas behaves as a collisional fluid and responds to nongravitational perturbations such as shocks, radiation pressure, or magnetic fields. Despite these potential complications, gas-dynamical models have been applied to a number of elliptical galaxies with circumnuclear gas disks (Harms et al. 1994; Ferrarese, Ford, & Jaffe 1996; Macchetto et al. 1997; van der Marel & van den Bosch 1998; Bower et al. 1998; Ferrarese & Ford 1999; Verdoes Kleijn et al. 2000).

Our group has concentrated on using STIS to apply the gas-dynamical technique to the bulges of spiral and S0 galaxies (Shields et al. 2000; Barth et al. 2001; Sarzi et al. 2001, 2002). Our work has revealed a subtlety that has not been widely appreciated in previous studies: the majority (~80%) of randomly chosen disk galaxies do *not* have well-behaved velocity fields suitable for gas-dynamical modeling at *HST* resolution. Based on this experience, we have developed an efficient strategy to preselect galaxies that significantly increases the chance of success for future STIS programs. This paper describes our technique, which is based on the use of the dust morphology to predict the velocity field.

¹ Based on observations made with the *Hubble Space Telescope*, which is operated by AURA, Inc., under NASA contract NAS5-26555.

² The Observatories of the Carnegie Institution of Washington, 813 Santa Barbara St., Pasadena, CA 91101; lho@ociw.edu.

³ Max-Planck-Institut für Astronomie, Königstuhl 17, Heidelberg, D-69117, Germany; rix@mpia-hd.mpg.de.

⁴ Dipartimento di Astronomia, Università di Padova, Vicolo dell'Osservatorio 5, I-35122 Padova, Italy; sarzi@pd.astro.it.

⁵ Physics & Astronomy Department, Ohio University, Athens, OH 45701; shields@phy.ohiou.edu.

⁶ Steward Observatory, Univ. of Arizona, Tucson, AZ 85721; grudnick@as.arizona.edu.

⁷ Department of Astronomy, University of California, Berkeley, CA 94720-3411; alex@astro.berkeley.edu.

⁸ Harvard-Smithsonian Center for Astrophysics, 60 Garden Street, Cambridge, MA 02138; abarth@cfa.harvard.edu.

⁹ California Institute of Technology, Dept. of Astronomy, 105-24, Pasadena, CA 91125.

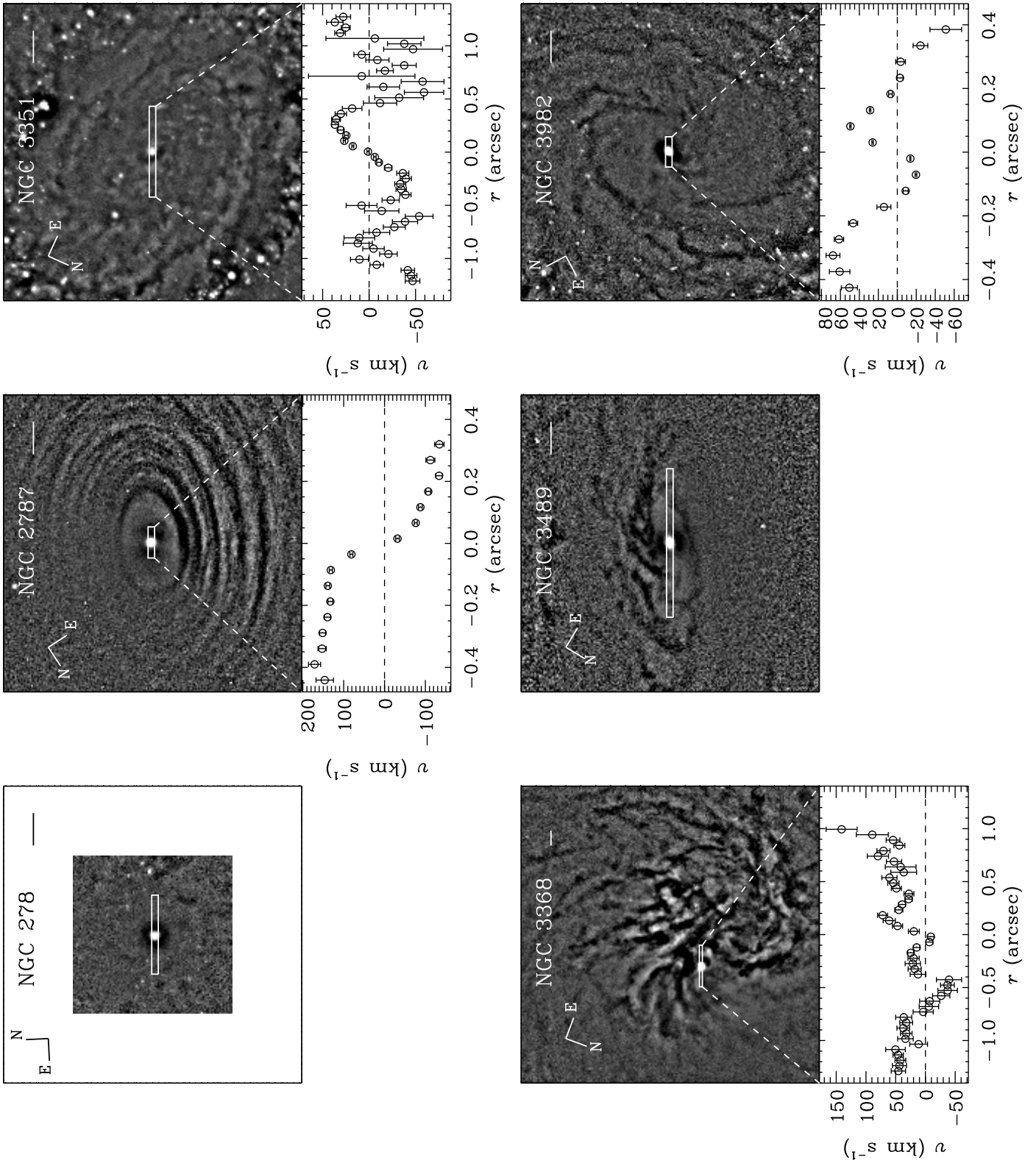


FIG. 1a.— Dust morphology and gas kinematics for NGC 278, 2787, 3351, 3368, 3489, and 3982. For each galaxy, the *top* panel shows the unsharp-masked, central $9''.1 \times 9''.1$ region of either a V-band WFPC2 image or the F28X50LP STIS acquisition image. (For NGC 3368, the image is a $20'' \times 20''$ section of the WF2 chip.) The horizontal bar on the upper right corner gives the scale of $1''$. The rectangular region superposed on the nucleus outlines the position of the slit. The *bottom* panel shows the H α velocity curve of the central $\sim 0''.5$ – $1''.0$, where the rest-frame velocity of the galaxy was determined by centering the rotation curve on the peak of the stellar continuum. The velocity curve is omitted for galaxies lacking extended emission.

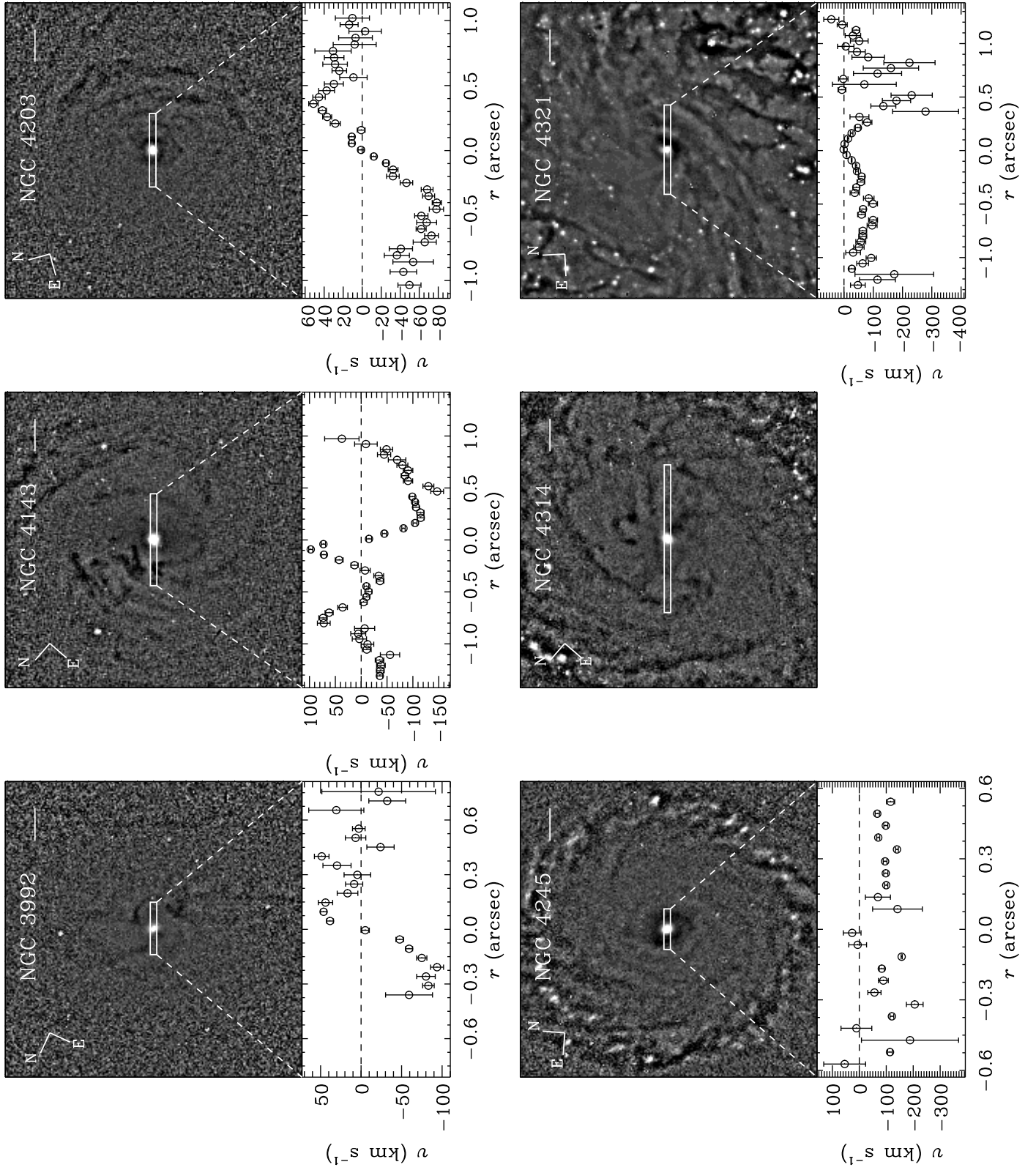


FIG. 1b.— Dust morphology and gas kinematics for NGC 3992, 4143, 4203, 4245, 4314, and 4321. As in Figure 1a.

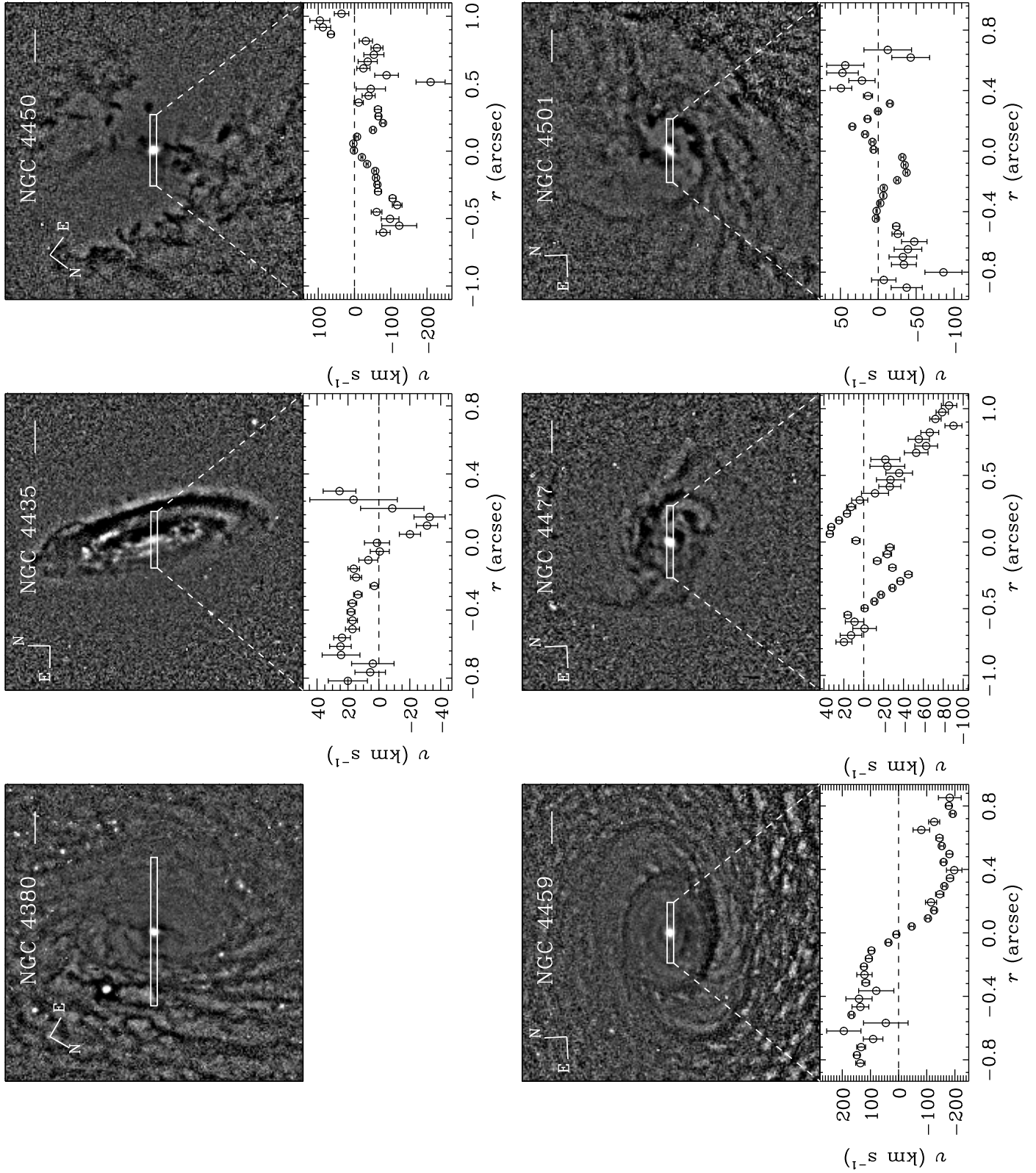


FIG. 1c.— Dust morphology and gas kinematics for NGC 4380, 4435, 4450, 4459, 4477, and 4501. As in Figure 1a.

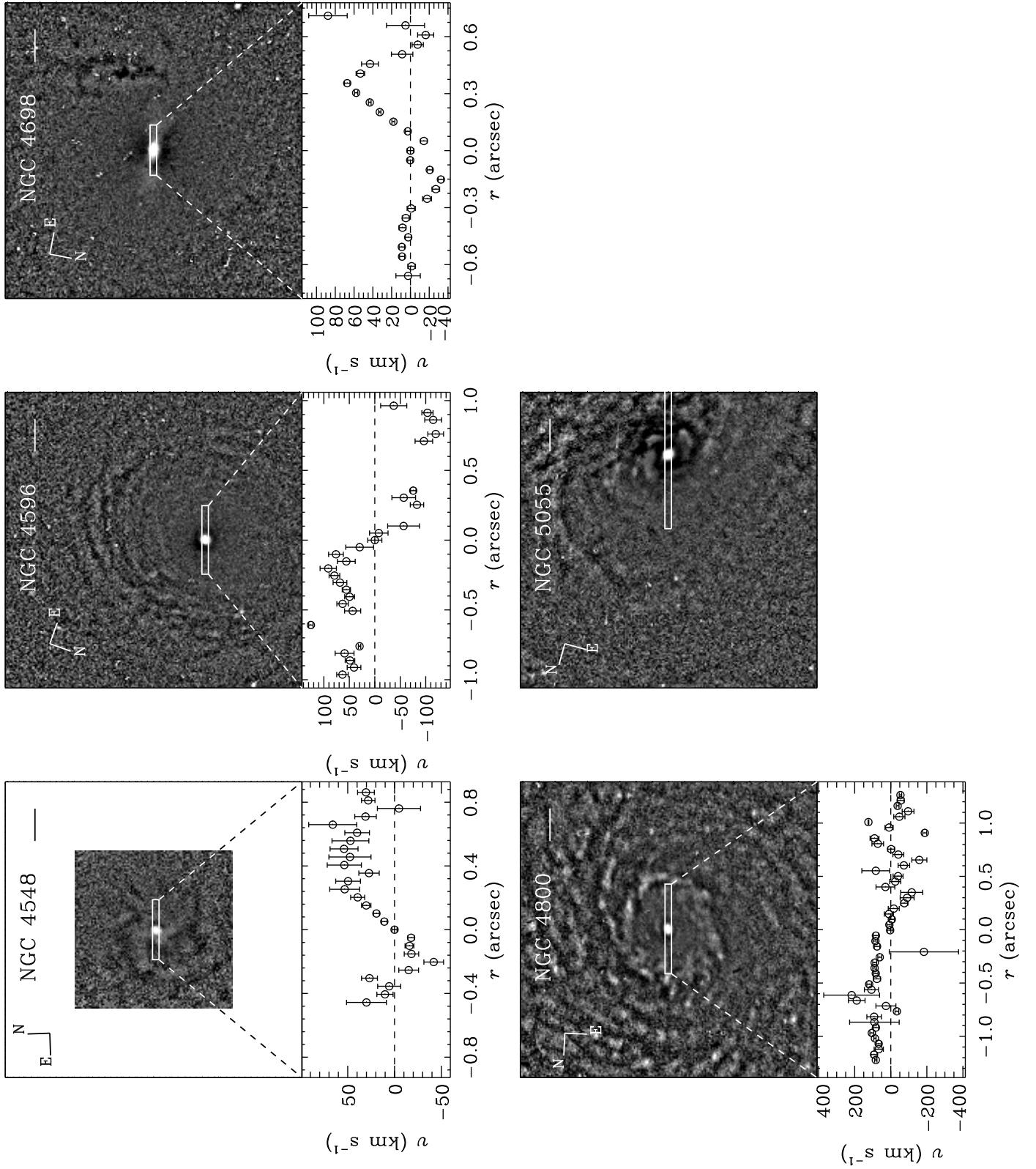


FIG. 1d.— Dust morphology and gas kinematics for NGC 4548, 4596, 4698, 4800, and 5055. As in Figure 1a.

TABLE 1
THE SAMPLE

Galaxy Name	Hubble Type	T	P.A. (deg.)	i (deg.)	D (Mpc)
(1)	(2)	(3)	(4)	(5)	(6)
NGC 278	SABb	3.0	11.8
NGC 2787	SB0+	-1.0	117	51	13.0
NGC 3351	SBb	3.0	13	48	8.1
NGC 3368	SABab	2.0	5	47	8.1
NGC 3489	SAB0+	-1.0	70	56	6.4
NGC 3982	SABb:	3.0	...	30	17.0
NGC 3992	SBbc	4.0	68	53	17.0
NGC 4143	SAB0	-2.0	144	52	17.0
NGC 4203	SAB0-:	-3.0	10	21	9.7
NGC 4245	SB0/a:	0.0	...	41	9.7
NGC 4314	SBa	1.0	...	27	9.7
NGC 4321	SABbc	4.0	30	32	16.8
NGC 4380	Sb?	3.0	153	58	16.8
NGC 4435	SB0	-2.0	13	44	16.8
NGC 4450	Sab	2.0	175	43	16.8
NGC 4459	S0+	-1.0	110	41	16.8
NGC 4477	SB0?	-2.0	15	24	16.8
NGC 4501	Sb	3.0	140	59	16.8
NGC 4548	SBb	3.0	150	38	16.8
NGC 4596	SB0+	-1.0	135	43	16.8
NGC 4698	Sab	2.0	170	53	16.8
NGC 4800	Sb	3.0	25	43	15.2
NGC 5055	Sbc	4.0	105	56	7.2

NOTE.— Col. (1) Galaxy name. Col. (2) Hubble type. Col. (3) Morphological type index. Col. (4) Position angle of the major axis of the galaxy. Col. (5) Inclination angle of the galaxy. Col. (6) Adopted distance, based on $H_0 = 75 \text{ km s}^{-1} \text{ Mpc}^{-1}$. Data taken from Ho et al. 1997.

2. THE DATA

The data used in this paper derive from our Cycle 7 STIS program GO-7361. Since a full description of the observations and data reductions will be given elsewhere (Rix et al. 2002; see also Sarzi et al. 2001, 2002), here we only mention a few key points pertinent to the present discussion. Our sample was designed to address a diverse set of scientific goals, among them measurement of BH masses in bulges. It comprises nearly all northern, bright S0–Sb galaxies within 17 Mpc that are known to have nuclear emission in the spectroscopic catalog of Ho, Filippenko, & Sargent (1997). We avoided galaxies later than Sb because their bulges are expected to be faint or absent, and because their higher dust content may compromise our ability to center the narrow slit on the nucleus. To further ensure that the nucleus will be easily accessible, we eliminated galaxies more inclined than 60° . The visibility of the nucleus was also confirmed by inspection of WFPC2 images, which were available for most of the galaxies. The final sample contained 24 galaxies, of which 23 (Table 1) were successfully observed; the acquisition of NGC 4138 failed because a nearby, bright star was mistaken for the nucleus.

Following a brief target-acquisition image using the F28X50LP long-pass filter, the primary kinematics data for each galaxy consist of a single-orbit integration with the G750M grating ($\lambda\lambda 6300\text{--}6870 \text{ \AA}$; FWHM $\Delta\lambda \approx 2.2 \text{ \AA}$) using the $0''.2 \times 52''$ slit. To enable flexibility in scheduling, we did not choose specific position angles for the slit.

3. DUST MORPHOLOGY AND VELOCITY FIELD

We detected $H\alpha$ and [N II] $\lambda\lambda 6548, 6583$ emission in all the objects, but the emission was symmetrically extended in the central $0''.5\text{--}1''.0$ in only $\sim 75\%$ (17/23) of the sample. For these 17 objects, “rotation curves” were derived from the radial velocities of the gas as a function of position along the slit using the $H\alpha$ and [N II] emission lines. The velocities of these features were derived using SPECFIT (Krisz 1994) within IRAF⁹, assuming a common velocity, a Gaussian profile, and a fixed [N II] doublet ratio of 3:1. The results are shown in Figure 1. A striking result is the rarity of galaxies with well-behaved velocity fields. Among the 17 galaxies with spatially resolved velocity profiles, only four (NGC 2787, 4203, 4459, 4596), or 25%, show ordered rotation curves amenable to dynamical analysis (Sarzi et al. 2001). The rest of the velocity curves look disorganized and difficult to interpret (Fig. 1). In terms of using the data for BH searches, therefore, the success rate is disappointingly low.

The greyscale panels in Figure 1 display the unsharp-masked optical continuum image of each galaxy. Most of the data are archival broad-band (roughly V) images acquired with the PC detector on WFPC2; two are our own STIS F28X50LP target-acquisition images. To accentuate high-spatial frequency features such as star clusters and dust lanes, we subtracted from each image a version of itself smoothed by a Gaussian with $\sigma = 4$ pixels ($\sim 0''.2$). The nucleus, by design, is clearly visible in each image. As was known from previous *HST* imaging studies of disk galaxies (Phillips et al. 1996; Carollo et al. 1997), dust is ubiquitous. Every galaxy in our sample shows dust lanes at some level within a central radius of $\sim 5''$, or ~ 400 pc for a typical distance of 17 Mpc. However, unlike the case of early-type (E and S0) galaxies (van Dokkum & Franx 1995; Tomita et al. 2000; Tran et al. 2001), the dust distributions do not resemble simple disks with sharply delineated, outer edges. Instead, the dust morphology can be best described as nuclear spirals (e.g., NGC 3351, NGC 3982), concentric rings (e.g., NGC 2787, NGC 4596), or simply chaotic (e.g., NGC 3368, NGC 4450). The one object with a fairly well-defined nuclear disk, NGC 4435, turns out to be an S0 galaxy.

Closer examination of the data reveals that the degree of “orderliness” of the gas kinematics evidently correlates with the morphology of the dust lanes. All four galaxies with well-behaved velocity fields (NGC 2787, 4203, 4459, 4596) have relatively smooth, circularly symmetric dust rings. The converse seems to hold for most, but not all, objects. For example, the dust patterns in NGC 4245 and NGC 4800 resemble those in the above-mentioned four objects, but neither has a regular, symmetric velocity field in ionized gas. The case of NGC 4435 deserves special remark. Although this galaxy possesses a clean nuclear disk, we were unable to obtain a usable symmetric rotation curve because the slit fell near the minor axis of its highly inclined disk (Fig. 1c). The velocity curve of the far side of the disk indeed looks regular, but that of the near side is obstructed by a prominent dust lane.

Thus, in terms of planning for *HST* BH searches using gas kinematics, it appears that *the morphology of the dust lanes can be used as an efficient and relatively reliable predictor of the gas kinematics*. Albeit somewhat subjective, and by no means perfectly foolproof, the strategy we advocate is nonetheless a highly effective tool for culling promising targets for STIS

⁹ IRAF is distributed by the National Optical Astronomy Observatories, which are operated by the Association of Universities for Research in Astronomy, Inc., under cooperative agreement with the National Science Foundation.

spectroscopy. It is especially attractive in view of the extensive database of optical images of nearby galaxies available in the *HST* archives and the straightforward manner in which unsharp masking can be performed on them. It would be fruitful to revisit these issues in the future when we have available images and spectra with resolutions higher than that currently possible with *HST*.

4. SUMMARY

Searches for massive BHs in bulges of disk galaxies generally must rely on gas-dynamical methods because these objects are dusty. Our experience with STIS data indicates that the success rate will be low in randomly chosen samples of spiral and S0 galaxies because well-defined nuclear gas disks with regular, symmetric velocity fields are rare in these objects. We show that the degree of regularity in the velocity field correlates with the morphology of the dust lanes, which can be efficiently as-

certained through unsharp masking of optical continuum *HST* images. Objects with smooth, circularly symmetric dust lanes tend to have velocity fields that are amenable to dynamical analysis. By contrast, galaxies with obviously disorganized dust morphology will almost never yield easily interpretable velocity fields. We draw attention to this empirical correlation as a powerful tool to select targets for future *HST* programs to search for massive BHs using gas kinematics.

This work was supported financially through NASA grant NAG 5-3556, and by grants in support of *HST* programs GO-7361 and GO-7403, awarded by STScI, which is operated by AURA, Inc., for NASA under contract NAS5-26555. Research by A. J. B. is supported by a postdoctoral fellowship from the Harvard-Smithsonian Center for Astrophysics. A. V. F. is grateful for a Guggenheim Foundation Fellowship."

REFERENCES

- Bacon, R., Emsellem, E., Combes, F., Copin, Y., Monnet, G., & Martin, P. 2001, *A&A*, 371, 409
- Barth, A. J., Sarzi, M., Rix, H.-W., Ho, L. C., Filippenko, A. V., & Sargent, W. L. W. 2001, *ApJ*, 555, 685
- Bower, G. A., et al. 1998, *ApJ*, 492, L111
- Carollo, C. M., Stiavelli, M., de Zeeuw, P. T., & Mack, J. 1997, *AJ*, 114, 2366
- Cretton, N., & van den Bosch, F. C. 1999, *ApJ*, 514, 704
- Ferrarese, L., & Ford, H. C. 1999, *ApJ*, 515, 583
- Ferrarese, L., Ford, H. C., & Jaffe, W. 1996, *ApJ*, 470, 444
- Ferrarese, L., & Merritt, D. 2000, *ApJ*, 539, L9
- Gebhardt, K., et al. 2000a, *AJ*, 119, 1157
- . 2000b, *ApJ*, 539, L13
- Harms, R. J., et al. 1994, *ApJ*, 435, L35
- Ho, L. C. 1999, in *Observational Evidence for Black Holes in the Universe*, ed. S. K. Chakrabarti (Dordrecht: Kluwer), 157
- Ho, L. C., Filippenko, A. V., & Sargent, W. L. W. 1997, *ApJS*, 112, 315
- Kormendy, J., & Bender, R. 1999, *ApJ*, 522, 772
- Kriss, G. A. 1994, in *Astronomical Data Analysis Software and Systems III*, ed. D. R. Crabtree, R. J. Hanisch, & J. Barnes (San Francisco: ASP), 437
- Leitherer, C., et al. 2001, *STIS Instrument Handbook, Version 5.1* (Baltimore: STScI)
- Macchetto, F., Marconi, A., Axon, D. J., Capetti, A., Sparks, W. B., & Crane, P. 1997, *ApJ*, 489, 579
- Phillips, A. C., Illingworth, G. D., MacKenty, J. W., & Franx, M. 1996, *AJ*, 111, 1566
- Richstone, D. O., et al. 1998, *Nature*, 395, A14
- Rix, H.-W., et al. 2002, in preparation
- Sarzi, M., Rix, H.-W., Shields, J. C., McIntosh, D. H., Ho, L. C., Rudnick, G., Filippenko, A. V., Sargent, W. L. W., & Barth, A. J. 2002, *ApJ*, submitted
- Sarzi, M., Rix, H.-W., Shields, J. C., Rudnick, G., Ho, L. C., McIntosh, D. H., Filippenko, A. V., & Sargent, W. L. W. 2001, *ApJ*, 550, 65
- Shields, J. C., Rix, H.-W., McIntosh, D. H., Ho, L. C., Rudnick, G., Filippenko, A. V., Sargent, W. L. W., & Sarzi, M. 2000, *ApJ*, 534, L27
- Tomita, A., Aoki, K., Watanabe, M., Takata, T., & Ichikawa, S. 2000, *AJ*, 120, 123
- Tran, H. D., Tsvetanov, Z., Ford, H. C., Davies, J., Jaffe, W., van den Bosch, F. C., & Rest, A. 2001, *AJ*, 121, 2928
- van der Marel, R. P., Cretton, N., de Zeeuw, P. T., & Rix, H.-W. 1998, *ApJ*, 493, 613
- van der Marel, R. P., & van den Bosch, F. C. 1998, *AJ*, 116, 2220
- van Dokkum, P. G., & Franx, M. 1995, *AJ*, 110, 2027
- Verdoes Kleijn, G. A., van der Marel, R. P., Carollo, C. M., & de Zeeuw, P. T. 2000, *AJ*, 120, 1221